A Non-Exponential Transmittance Model for Volumetric Scene Representations – Supplemental Material

DELIO VICINI, Facebook Reality Labs and École Polytechnique Fédérale de Lausanne (EPFL), Switzerland
WENZEL JAKOB, École Polytechnique Fédérale de Lausanne (EPFL), Switzerland
ANTON KAPLANYAN, Facebook Reality Labs, USA

1 RELATION TO VOLTERRA INTEGRAL FORMULATION

For an exponential transmittance, i.e. $f(\tau) = \exp(-\tau)$, our integral formulation matches the Volterra integral used by Georgiev et al. [2019]. Their formulation was derived directly from the RTE, instead of just using calculus. However, it can be transformed into ours as follows:

$$\begin{aligned} \mathrm{T}(\mathbf{x}, \mathbf{y}) &= 1 - \int_0^{\|\mathbf{x}-\mathbf{y}\|} \mathrm{T}(\mathbf{x}, \mathbf{x} + \boldsymbol{\omega} t)\sigma_t(t)\, \mathrm{d}t \\ &= 1 - \int_0^{\|\mathbf{x}-\mathbf{y}\|} e^{-\int_0^t \sigma_t(s)\, ds} \sigma_t(t)\, \mathrm{d}t \\ &= 1 + \int_0^{\|\mathbf{x}-\mathbf{y}\|} \frac{\partial f}{\partial \tau}\left(\int_0^t \sigma_t(s)\, \mathrm{d}s\right) \sigma_t(t)\, \mathrm{d}t \qquad (1) \\ &= 1 + \int_0^{\|\mathbf{x}-\mathbf{y}\|} \frac{\partial f}{\partial \tau}\left(f^{-1}(\mathrm{T}(\mathbf{x}, \mathbf{x}_t))\right) \sigma_t(t)\, \mathrm{d}t. \qquad (2) \end{aligned}$$

Their paper then uses the Taylor series of the exponential function to write the transmittance as an infinite sum. It turns out that recursively expanding a function using the fundamental theorem of calculus is one of several ways to derive the Taylor series of a function in the first place.

2 RAY MARCHING ALGORITHM

We use ray marching to estimate the transmittance by our model. Our transmittance model was defined to be:

$$\mathrm{T}(\mathbf{x}, \mathbf{y}) = 1 + \int_0^{\|\mathbf{x}-\mathbf{y}\|} \frac{\partial f}{\partial \tau}\left(f^{-1}\left(\mathrm{T}(\mathbf{x}, \mathbf{x}_t), \gamma(t)\right), \gamma(t)\right) \sigma_{\mathrm{t}}(t)\, \mathrm{d}t \qquad (3)$$

To evaluate the transmittance, we need to approximate the value of this integral. We can do that by applying a Riemann summation:

$$\mathrm{T}(\mathbf{x}, \mathbf{y}) \approx 1 + \sum_{i=1}^{N} \frac{\partial f}{\partial \tau}\left(f^{-1}\left(\mathrm{T}_{i-1}, \gamma(t_i)\right), \gamma(t_i)\right) \sigma_{\mathrm{t}}(t_i)\Delta_{\mathrm{step}} \qquad (4)$$

where for convenience we defined the transmittance after $i - 1$ steps in the summation as T_{i-1} (with $\mathrm{T}_0 = 1$). However, if one tries to use this formulation one encounters an issue. Our transmittance model was derived using the fundamental theorem of calculus, but the fundamental theorem of calculus does not hold under a basic Riemann summation. This can be fixed by also using a discrete version of the derivative term in the integrand. We use a finite difference approximation with the step size of $\sigma_{\mathrm{t}}\Delta_{\mathrm{step}}$:

$$\frac{\partial f}{\partial \tau}(\tau, \gamma) \approx \frac{1}{\sigma_{\mathrm{t}}\Delta_{\mathrm{step}}}\left[f(\tau + \sigma_{\mathrm{t}}\Delta_{\mathrm{step}}, \gamma) - f(\tau, \gamma)\right] \qquad (5)$$

Using the extinction as the finite difference offset is convenient, as the division by it will then cancel out with the $\sigma_{\mathrm{t}}\Delta_{\mathrm{step}}$ term in the original Riemann sum:

$$\begin{aligned} \mathrm{T}(\mathbf{x}, \mathbf{y}) &\approx 1 + \sum_{i=1}^{N} \Big[f\left(f^{-1}(\mathrm{T}_{i-1}, \gamma(t_i)) + \sigma_{\mathrm{t}}(t_i)\Delta_{\mathrm{step}}, \gamma(t_i)), \gamma(t_i)\right) \\ &\qquad - f\left(f^{-1}(\mathrm{T}_{i-1}, \gamma(t_i)), \gamma(t_i)\right) \Big] \\ &= 1 + \sum_{i=1}^{N} f\left(f^{-1}(\mathrm{T}_{i-1}, \gamma(t_i)) + \sigma_{\mathrm{t}}(t_i)\Delta_{\mathrm{step}}, \gamma(t_i)\right) - \mathrm{T}_{i-1} \end{aligned} \qquad (6)$$

In the last step, we arrive at a telescoping sum. This means that we can also write the ray marching algorithm as a simple recursive function:

$$\mathrm{T}(\mathbf{x}, \mathbf{y}) \approx f\left(f^{-1}\left(\mathrm{T}_{N-1}, \gamma(t_i)\right) + \sigma_{\mathrm{t}}(t_i)\Delta_{\mathrm{step}}, \gamma(t_i)\right) \qquad (7)$$

Each iteration in the ray marching algorithm then updates the value of T based on its previous value and the current values for σ_{t} and γ.

3 INVERSE TRANSMITTANCE KERNEL

To evaluate our heterogeneous transmittance model, we need to compute the inverse of the transmittance kernel $f(\tau, \gamma)$ with respect to its first argument. The simple form of f allows to write the inverse explicitly using the Lambert W function:

$$f^{-1}(y, \gamma) = \begin{cases} 2 - 2y & \gamma = 0 \\ -\log(y/\gamma) & \gamma \exp(-2) > y \\ 2\frac{y+\gamma-1}{\gamma-1} + W\left[-2\gamma \exp\left(-2\frac{y+\gamma-1}{\gamma-1}\right)\right] & \gamma \exp(-2) \leq y \end{cases}. \qquad (8)$$

Being able to compute the inverse transmittance function is not only necessary to evaluate our transmittance formulation, but also allows to efficiently optimize the medium parameters using gradient descent.

Authors' addresses: Delio Vicini, delio.vicini@epfl.ch, Facebook Reality Labs and École Polytechnique Fédérale de Lausanne (EPFL), Lausanne, Switzerland; Wenzel Jakob, wenzel.jakob@epfl.ch, École Polytechnique Fédérale de Lausanne (EPFL), Lausanne, Switzerland; Anton Kaplanyan, kaplanyan@gmail.com, Facebook Reality Labs, Redmond, USA.

4 RECIPROCITY

Our model does not enforce reciprocity. While we provide some results in the main paper, we show some additional evaluation in Figure 1.

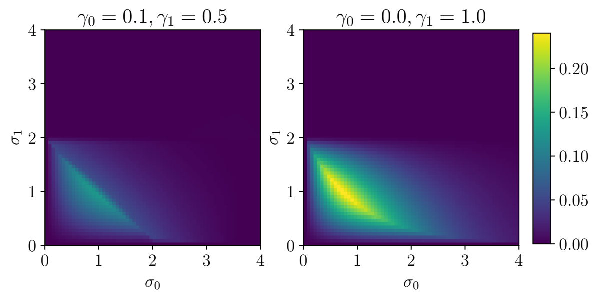

Fig. 1. In this figure, we plot the absolute difference between evaluating the transmittance across two voxels from either direction. The error depends on the medium parameters σ_t and γ. We show two plots over the extinction values of the two voxels, each for different settings of transmittance modes. The difference is maximized if the two adjacent voxels have completely opposite transmittance modes ($\gamma_0 = 0$ and $\gamma_1 = 1$), and gets smaller as the difference in transmittance mode decreases. If both voxels have the same transmittance mode, the difference goes to zero. The error also goes to zero as the voxels become either fully transparent or fully opaque.

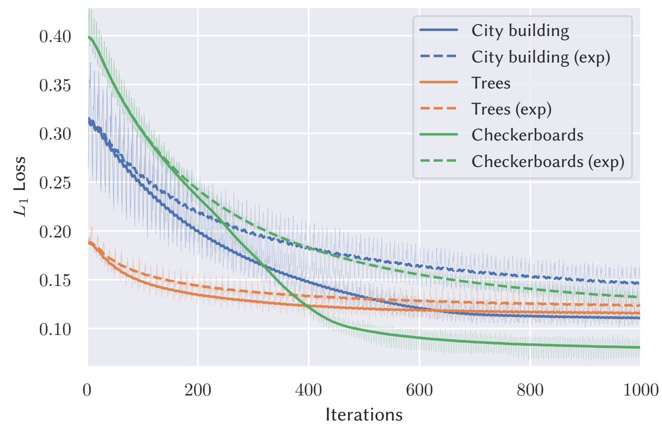

Fig. 2. Convergence plot of the L_1 loss during optimization across different scenes at a resolution of 64^3. The thick lines represent the loss values averaged across 40 iterations. We found the convergence behavior to be fairly uniform across all the scenes and resolutions we tested.

5 OPTIMIZATION CONVERGENCE

The optimization convergence for prefiltering multiple scenes is shown in Figure 2. It is fairly uniform and does not suffer from saddle points. The loss achieved using our non-exponential model is significantly lower for scenes with many opaque surfaces (such as "Checkerboards" and "City building"), while performing comparably to the exponential model for aggregate scenarios (such as "Trees" scene). This is expected, as our model is targeted at improving the representation of scenes with opaque surfaces.

6 VOLUME ACCESS STATISTICS

In the following table we provide additional statistics on the amount of voxel data accessed at render time. This shows that a sparse voxelization of the scene scales favorably as the resolution increases.

Resolution	16	32	64	128
City building	153.1	204.9	231.1	257.2
City	97.7	102.6	128.3	161.0
Trees	122.9	177.9	242.5	283.9
Checkerboards	230.2	291.9	288.8	310.4
Fractal	269.1	347.8	474.4	532.7
Plane	126.5	125.9	152.1	150.1

Table 1. The amount of non-empty voxel data accessed per sample for different scenes and resolutions. The reported numbers are average number of bytes accessed while rendering different views of the scene. The data is measured *per sample*, using multiple scattering and next event estimation. These measurements show that the growth in data access size is sublinear as the volume resolution increases.

REFERENCES

Iliyan Georgiev, Zackary Misso, Toshiya Hachisuka, Derek Nowrouzezahrai, Ja roslav Křivánek, and Wojciech Jarosz. 2019. Integral formulations of volumetric transmittance. *ACM Trans. Graph. (Proc. SIGGRAPH Asia)* 38, 6 (2019), 17 pages.